State-space modeling of fatigue crack growth in ductile alloys[☆]

Ravindra Patankar, Asok Ray*

Mechanical Engineering Department, The Pennsylvania State University, University Park, PA 16802, USA

Abstract

This paper presents a nonlinear dynamical model of fatigue crack growth in ductile alloys under variable-amplitude loading. The model equations are formulated in the state-space setting based on the crack closure concept and capture the effects of stress overload and reverse plastic flow. The state variables of the model are crack length and crack opening stress. The constitutive equation of crack-opening stress in the state-space model is governed by a low-order nonlinear difference equation that does not require storage of a long load history. The state-space model can be restructured as an autoregressive moving average (ARMA) model for real-time applications such as health monitoring and life extending control. The model is validated with fatigue test data for different types of variable-amplitude and spectrum loading including single-cycle overloads, irregular sequences, and random loads in 7075-T6 and 2024-T3 alloys. Predictions of the state-space model are also compared with those of the FASTRAN-II model. © 2000 Elsevier Science Ltd. All rights reserved.

Keywords: Fatigue and fracture; State-space modeling; Sequence effects; Spectrum loading

1. Introduction

This paper presents a nonlinear dynamical model of fatigue crack growth under variable-amplitude loading in ductile alloys following the state-space approach. The proposed model, hereafter referred to as the state-space model, is formulated based on the crack closure concept where the state variables are the crack length a and the crack-opening stress S^o. The crack growth equation in the state-space model

* Corresponding author. Tel: +1-814-865-6377; fax: +1-814-863-4848.
 E-mail address: axr2@psu.edu (A. Ray).

Nomenclature

A_k^j	parameter in the empirical equation of S_k^{oss} for $j = 1, 2, 3, 4$
a	crack length
C	parameter in the crack growth equation
E	Young's modulus
$F(\cdot, \cdot)$	crack length dependent geometry factor
$h(\cdot)$	crack growth function in crack growth equation
k	current cycle of stress excitation
ℓ	crack growth retardation delay in cycles
m	exponent parameter in the crack growth equation
m	number of cycles of a particular stress level in the load block
n	number of cycles of a particular stress level in the load block
R	stress ratio of minimum stress to maximum stress
S^{flow}	flow stress
S^{max}	maximum stress within a cycle
S^{min}	minimum stress within a cycle
S^o	crack opening stress
S^{oss}	crack opening stress under constant amplitude load given by empirical equation.
S^{ult}	ultimate tensile strength
S^y	yield stress
t	specimen thickness
$U(\cdot)$	the Heaviside function
w	half-width of center-cracked specimen or width of compact specimen
α	constraint factor for plane stress/strain
α^{max}	maximum value of α
α^{min}	minimum value of α
Δa^{max}	crack increment above which $\alpha = \alpha^{min}$
Δa^{min}	crack increment below which $\alpha = \alpha^{max}$
Δa_k	crack increment ($= a_k - a_{k-1}$)
ΔK^{eff}	effective stress intensity factor range
ε^{thr}	positive lower bound for absolute value of maximum stress $\{S_k^{max}, k \geq 0\}$.
η	decay rate for S^o
$\Re$	the set of real numbers $(-\infty, \infty)$
τ	time instant
$\Im$	time interval of a cycle

is structurally similar to Paris equation [1] modified for crack closure, which has been extensively used in fatigue crack growth models such as FASTRAN-II [2] and AFGROW [3]. Under variable-amplitude loading, these models usually rely on a memory-dependent physical variable (e.g., crack opening stress, or reference stress) that requires storage of information on the load history. For example, the crack-opening stress in the FASTRAN-II model [2] is assumed to depend on the load history over an interval of about 300 cycles. Another example is the strain-life model in which the reference stress obtained by the rainflow method relies on cycle counting that, in turn, depends on the load history [4,5]. In the current state of the art of fatigue crack growth modeling, the finite interval over which the load history is considered to be relevant may vary with the type of loading as well as with the rules employed for

cycle counting. The model predictions, in general, become more accurate if the load history is considered over a longer period although a short recent history of the applied load might be adequate for crack growth modeling in some cases. An extreme example is constant-amplitude cyclic loading where storage of the load history over the previous cycles may not be necessary. In essence, it is not precisely known to what extent information storage is necessary for calculating the memory-dependent variable in a fatigue crack growth model under a priori unknown variable-amplitude (e.g., single-cycle, block, spectrum, or random) loading. Nevertheless, this memory-dependent variable can be modeled in a finite-dimensional state-space setting by an ordinary difference (or differential) equation. The state at the current cycle is realized as a combination of the state and the input (i.e., cyclic stress) excitation at finitely many previous cycles. Equivalently, the state becomes a function of the fading memory of the input excitation, which can be generalized to an autoregressive moving average (ARMA) model that is equivalent to a state-space model [6]. Unlike the existing crack growth models (e.g., [7,8]), the state-space model does not require a long history of stress excitation to calculate the crack-opening stress. Therefore, savings in the computation time and memory requirement are significant.

The state-space model adopts a novel approach to generate the (cycle-dependent) crack opening stress S_k^o under variable-amplitude loading, while the structure of its crack growth equation is similar to that of FASTRAN-II [2]. As such, the crack length computed by these two models could be different under a given variable amplitude loading, although the results are essentially identical under the same constant-amplitude loading. The state-space model is formulated to satisfy the following requirements:

1. Capability to capture the effects of single-cycle overload and underload, load sequencing, and spectrum loading;
2. Representation of physical phenomena of fracture mechanics within a semi-empirical structure;
3. Compatibility with dynamic models of operating plants for health monitoring and life extending control;
4. Validation by comparison with fatigue test data and another well-known code of fatigue crack growth;
5. Development of a computer code using standard languages for real-time execution on standard platforms.

The requirements #1 and #2 are satisfied as the state-space model is formulated based on fracture-mechanistic principles of the crack closure concept. The requirement #3 is also satisfied because the plant dynamic models are usually formulated in the state-space setting or ARMA setting [6]. The remaining two requirements, #4 and #5, are satisfied by validating the state-space model with fatigue test data for different types of variable-amplitude and spectrum loading on 7075-T6 and 2024-T3 alloys [9,10], respectively. The model predictions are also compared with those of FASTRAN-II, which is a well-known code for fatigue crack growth prediction and is widely used in the aircraft industry. While the results derived from the state-space and FASTRAN-II models are comparable, the state-space model enjoys significantly smaller computation time and memory requirements as needed for real-time execution on standard platforms such as a Pentium PC. This is because the state-space model is described by a low-order difference equation, and therefore, does not need for storage of a long load history. This simple structure of the state-space model facilitates the task of code generation and verification using standard high-level programming languages.

This paper is organized in five sections including the present section. Section 2 formulates the model equations in the state-space setting based on fracture-mechanistic principles and delineates the features of the state-space model including its response characteristics under overload and underload excitation. Section 3 validates the state-space model by comparison with fatigue test data under different types of variable-amplitude loading including spectral loading for 7075-T6 and 2024-T3 aluminum alloys, as well as with the predictions of the FASTRAN-II model under identical load excitation. Section 4 compares

execution time and memory requirements of the state-space model with those of the FASTRAN-II model for load profiles. Section 5 summarizes and concludes the paper with recommendations for future research.

2. Formulation of the crack growth model in state-space setting

The state-space model of crack growth is formulated based on mechanistic principles of the crack-closure concept and is supported by fatigue test data for variable-amplitude cyclic loading (e.g., [9–11]). The following definition of a fatigue cycle is adopted for model development in the sequel:

Definition 2.1. The kth fatigue cycle is defined on the time interval:

$$\mathfrak{I}_k = \left\{ \tau \in \mathfrak{R} : \underline{\tau}_{k-1} < \tau \leq \underline{\tau}_k \right\} \quad \text{with } \underline{\tau}_{k-1} < \bar{\tau}_k < \underline{\tau}_k$$

where $\mathfrak{R} \equiv (-\infty, \infty)$ is the set of real numbers; $\underline{\tau}_k$ and $\bar{\tau}_k$ are the time instants of occurrence of the minimum stress $S_k^{\min}$ and the maximum stress $S_k^{\max}$, respectively. The kth fatigue cycle is denoted as the ordered pair $(S_k^{\max}, S_k^{\min})$.

Remark 2.1. *A stress cycle is determined by the maximum stress S^{max} and the following minimum stress S^{min}. The frequency and the shape of a stress cycle are not relevant for crack growth in ductile alloys at room temperature [12]. The load dependence of crack growth is assumed to be completely characterized by peak and valleys of applied stress at temperatures significantly below one third of the melting point (e.g. aluminum and ferrous alloys at room temperature). It follows from the above definition that $S_k^{\max} > \max(S_{k-1}^{\min}, S_k^{\min})$.*

Before proceeding to develop the fatigue crack growth model, pertinent observations that are critical for model formulation and validation are summarized below:

1. An overload may introduce significant crack growth retardation. Up to certain limits, the tenure of crack retardation effects is increased by:
   ○ larger magnitudes of the overload excitation;
   ○ periodic repetition of the overload during the crack propagation life; and
   ○ application of short blocks of overload instead of isolated single-cycle overloads.

2. Crack retardation may not always immediately follow the application of an overload. There could be a short delay before the crack growth rate starts decreasing. Under some circumstances, a small initial acceleration in crack growth has been observed. The delayed retardation in crack growth due to overload was clearly verified by observation of striation spacing [13].
3. The instantaneous crack growth caused by an overload itself is larger than that expected from a constant-amplitude load equal to the amplitude of the overload. This observation has been confirmed by fractography [10]. The rationale is that the crack opening stress S° picks up in magnitude a few cycles after application of the overload whereas, for constant amplitude load, S° is already at its steady-state value equal to S^{oss}. Therefore, the crack growth rate while S° is increasing due to a large $S^{\max}$ is higher than the rate when S° has the steady-state value S^{oss}.
4. An underload has smaller effects on crack growth than an overload of the same magnitude [9]. However, an underload applied immediately after an overload may significantly compensate for the effects of crack growth retardation due to the overload [9,14,15]. If the underload precedes the overload, the compensation is much smaller due to a sequence effect of the overload cycles.

5. In step loading, a high-low sequence produces qualitatively similar results as overload cycles including delayed retardation [13]. Interaction effects after a high-low sequence are barely detectable in the macroscopic sense. However, more accurate measurements and striations do reveal existence of locally accelerated crack growth according to McMillan and Pelloux [10].

6. Duration of crack growth retardation depends upon ductility of the material. If ductility of an alloy is modified by heat treatment, a lower (higher) yield strength corresponds to a longer (shorter) retardation period. Moreover, the specimen geometry also affects the retardation period. Schijve [11] tested specimens of different thickness under equivalent single-cycle overload conditions. A reduction in retardation period was observed with increase in thickness.

7. Rest periods at zero stress following a tensile peak overload have no significant influence on subsequent fatigue crack retardation for ductile alloys at room temperature [16].

8. The approximate non-minimum phase behavior of crack opening stress, observed by Yisheng and Schijve [17] and Newman [18], is explained as follows: Upon application of an overload, S^{o} decreases sharply and then rapidly undergoes an overshoot followed by a slow decay. Similarly, an underload would cause a sharp increase in S^{o} before an undershoot is observed. Debayeh and Topper [19] measured crack-opening stress on 2024-T351 aluminum alloy specimens using 900 power short focal length optical microscope at 1, 5, 10, 50, 100 cycles, immediately after application of an overload. The non-minimum phase behavior of S^{o} was not observed in any one of those specimens. Therefore, existence of the non-minimum phase behavior in the transient response of S^{o} is debatable at this moment. Since the transients having the non-minimum phase behavior, if they exist, are fast, their contributions to overall crack growth are considered to be insignificant relative to the total fatigue life.

Most fatigue crack growth models reported in technical literature are based on modifications of the Paris equation [1] in which the inputs are $S_k^{\max}$ and $S_k^{\min}$ in the kth cycle and the output is the crack length increment Δa_k. It is customary in the fracture mechanics community [12,20] to express the dynamical behavior of fatigue crack growth as a derivative $\mathrm{d}a/\mathrm{d}N$ with respect to the number of cycles, which is essentially Δa_k in the kth cycles as delineated below:

$$
\left.\begin{aligned}
\Delta a_k &\equiv a_k - a_{k-1} = h\big(\Delta K_k^{\mathrm{eff}}\big) \text{ with } h(0) = 0 \\
\Delta K_k^{\mathrm{eff}} &\equiv \sqrt{\pi a_{k-1}} F(a_{k-1}, w)\big(S_k^{\max} - S_{k-1}^{\mathrm{o}}\big) U\big(S_k^{\max} - S_{k-1}^{\max}\big)
\end{aligned}\right\} \text{ for } k \ge 1 \text{ and } a_0 > 0 \tag{1}
$$

where a_{k-1} and S_{k-1}^{o} are the crack-length and the crack-opening stress, respectively, during the kth cycle and change to a_k and S_k^{o} at the expiry of the kth cycle; $F(\cdot,\cdot)$ is a crack-length-dependent correction factor compensating for finite geometry of the specimen with the width parameter w; the non-negative monotonically increasing function $h(\cdot)$ can be represented either by a closed form algebraic equation, for example in the form $C(\Delta K_k^{\mathrm{eff}})^m$, or by table lookup [2]; and

$$
U(x) = \begin{cases} 0 & \text{if } x < 0 \\ 1 & \text{if } x \ge 0 \end{cases}
$$

is the Heaviside unit step function.

Eq. (1) is a first-order nonlinear difference equation excited by $S_k^{\max}$ and S_{k-1}^{o} in the kth cycle. Apparently, the crack length a_k can be treated as a state variable in Eq. (1). However, since S^{o} is dependent on the stress history (i.e., the ensemble of peaks $S^{\max}$ and valleys $S^{\min}$ in the preceding cycles). Eq. (1) cannot be readily represented in the state-space setting in its current form. The task is now to make a state-variable representation of the evolution of S^{o} under variable-amplitude cyclic stress excitation, and then augment the crack growth model in Eq. (1) with S^{o} as an additional state variable. It is postulated that a state-space model of crack growth is observable [21]. In other words, the state

variables in any given cycle can be determined from the history of measured variables over a finite number of cycles. The crack length a_k is assumed to be measurable. The other state variable, the crack-opening stress S^o, although not necessarily a measurable quantity, can be determined from a finite history of the input (i.e., peaks and valleys of stress excitation) and the output (i.e., crack length measurements), starting from a particular cycle in the past onwards to the current cycle. This concept is analogous to the methods used in the existing crack growth models where either the crack-opening stress or the reference stress is obtained based on the history of cyclic stress excitation.

It is observed from experimental data that S^o requires a short period of cycles to rise a peak value after the application of a single-cycle overload. If a first order difference equation is postulated to model the transient behavior of S^o, then S^o can be depicted to have an instantaneous rise, which is a good approximation for most ductile alloys. The application of an overload should generate a positive pulse to excite an appropriate state-space equation. Moreover, once this overload pulse reaches its peak, decay of S^o should be very slow. Hence, upon application of a large positive overload, the peak of S^o may be significantly larger than its steady-state value. Upon application of another small overload when S^o is still larger than its steady-state value, the smaller overload should not have any significant effect. In other words, a small overload following a large overload should not generate a pulse input to the state-space equation. This implies nonlinearity of the forcing function that can be captured by a Heaviside function. As the nonlinearity is dependent upon the current value of S^o, a low-order nonlinear difference equation can provide a viable model for describing the transient behavior of S^o under overload conditions.

The plastic zone size is largest during a load cycle when S^{max} is applied. As the applied stress is decreased from S^{max}, there is a reverse plastic flow at the crack tip [22]. The reverse plastic flow is at its maximum when the minimum stress S^{min}, even if positive in value; is applied. This reverse plastic flow depletes the large plastic zone caused by S^{max}. If the crack growth leads into a large overload-plastic zone and if an underload is applied next, then depletion of the plastic zone is higher than the one that would be caused by a regular (i.e., higher) S^{min}. This effect reduces the protection against crack growth, which can be stated in other terms as a decrease in S^o. Lardner [22] modeled an elastoplastic shear crack in which the crack was replaced by a linear array of freely slipping dislocations and the plastic zones by coplanar arrays moving against a frictional resistance.

Rainflow cycle counting [5] has been used in variable-amplitude fatigue models to generate the reference stress, which is analogous to the crack-opening stress to some extent. The rainflow technique remembers the stress history back to the occurrence of least minimum stress. If the new minimum stress is lower than the previous minimum stress, then cycles are counted according to a rule between these two minimum stresses and the stored stress profile is updated starting from the new minimum stress. This is analogous to encountering a new S^{min} that is lower than its past values. This new S^{min} causes a large reverse plastic displacement leading to severe depletion of the plastic zone, wherefrom it has to be built up again by continued application of the stress profile. When the plastic zone is severely depleted, the memory of the previous plastic zone is destroyed and a new memory is built up as the load is applied further on. The accurately predict the crack growth, the state-space model must be able to account for the entire reverse plastic flow.

We now proceed to determine the structure of the difference equation that is excited by the cyclic stress input to generate the crack opening stress. To this end, we first consider the steady-state solution of the difference equation under constant amplitude load. This issue has been addressed by several investigators including Newman [23] and Ibrahim et al. [24]. The steady-state crack-opening stress S^{oss} under a constant amplitude cyclic load is a function of the minimum stress S^{min}, the maximum stress S^{max}, the constraint factor α (which is 1 for plane stress and 3 for plane strain), the specimen geometry, and the flow stress S^{flow} (which is the average of the yield strength S^y and the ultimate strength S^{ult}).

These relationships are shown to be good for most ductile alloys by Newman [23]. One such empirical relation has been used in the FASTRAN-II model [2].

The objective is to construct the difference equation for (cycle-dependent and non-negative) crack opening stress S_k^{o} such that, under different levels of constant-amplitude load, the forcing function S_k^{oss} at the kth cycle matches the crack-opening stress derived from the following empirical relation [23] that is valid for tensile peak stress (i.e., $S_k^{\max} > 0$):

$$S_k^{\mathrm{oss}} = S^{\mathrm{oss}}\left(S_k^{\max}, S_k^{\min}, \alpha_k, F(a_{k-1}, w)\right)$$

$$\equiv \begin{cases} \left(\max\left\{\left(A_k^0 + A_k^1 R_k + A_k^2 (R_k)^2 + A_k^3 (R_k)^3\right), R_k\right\}\right) S_k^{\max} & \text{for } R_k \geq 0 \\ \left(A_k^0 + A_k^1 R_k\right) S_k^{\max} & \text{otherwise} \end{cases} \tag{2}$$

where

$$R_k = \frac{S_k^{\min}}{S_k^{\max}} U\left(S_k^{\max}\right) \quad \text{for all } k \geq 0; \tag{3}$$

$$A_k^0 = \left(0.825 - 0.34\alpha_k + 0.05(\alpha_k)^2\right)\left[\cos\left(\frac{\pi}{2}\frac{S_k^{\max}}{S^{\mathrm{flow}}} F(a_{k-1}, w)\right)\right]^{1/\alpha_k} \tag{4}$$

$$A_k^1 = (0.415 - 0.071\alpha_k)\left(\frac{S_k^{\max}}{S^{\mathrm{flow}}} F(a_{k-1}, w)\right) \tag{5}$$

$$A_k^2 = \left(1 - A_k^0 - A_k^1 - A_k^3\right) U(R_k) \tag{6}$$

$$A_k^3 = \left(2A_k^0 + A_k^1 - 1\right) U(R_k) \tag{7}$$

The constraint factor α_k used in Eqs. (4) and (5) is obtained as a function of the crack length increment Δa_k in Eq. (1) and a procedure for evaluation of α_k is presented in the FASTRAN-II manual [2]. Since α_k does not significantly change over cycles, it can be approximated as piecewise constant for limited ranges of crack length.

Remark 2.2. *It is possible to modify* Eq. (2) *for non-tensile peak stresses (i.e., $S_k^{\max} \leq 0$). The state-space model is not validated for $S_k^{\max} \leq 0$ due to unavailability of appropriate test data.*

Remark 2.3. *The inequality in the Heaviside function $U(S_k^{\max})$ of* Eq. (3) *should be realized by setting $S_k^{\max} \geq \varepsilon^{\mathrm{thr}} > 0$ to avoid the singular region around $S_k^{\max} = 0$. The parameter $\varepsilon^{\mathrm{thr}}$ is selected during code development. This modification is not necessary for applications where the peak stress is sufficiently tensile.*

The following constitutive relation in the form of a nonlinear first order difference equation is proposed for recursive computation of the crack-opening stress S_k^{o} upon the completion of the kth cycle [25]:

$$S_k^o = \left(\frac{1}{1+\eta}\right)S_{k-1}^o + \left(\frac{\eta}{1+\eta}\right)S_k^{oss} + \left(\frac{1}{1+\eta}\right)(S_k^{oss} - S_{k-1}^o)U(S_k^{oss} - S_{k-1}^o) + \left(\frac{1}{1+\eta}\right)[S_k^{oss}$$

$$- S_k^{oss\_old}]U(S_{k-1}^{min} - S_k^{min})[1 - U(S_k^{oss} - S_{k-1}^o)] \tag{8}$$

$$\eta = \frac{tS^y}{2wE} \tag{9}$$

where the forcing function S_k^{oss} in Eq. (8) is calculated from Eq. (2) as if a constant amplitude stress cycles (S_k^{max}, S_k^{min}) is applied; similarly, $S_k^{oss\_old}$ is given by Eq. (2) as if a constant amplitude stress cycle $(S_k^{max}, S_{k-1}^{min})$ is applied. For constant-amplitude loading, S^{oss} is the steady-state solution of S^o. In general, the inputs S_k^{oss} and $S_k^{oss\_old}$ to Eq. (8) are different from the instantaneous crack-opening stress S_k^o under variable-amplitude loading. The Heaviside function $U(S_k^{oss} - S_{k-1}^o)$ in the third term on the right-hand side of Eq. (8) allows fast rise and slow decay of S^o. The last term on the right-hand side of Eq. (8) accounts for the effects of reverse plastic flow. Depletion of the normal plastic zone occurs when the minimum stress S_k^{min} decreases below its value S_{k-1}^{min} in the previous cycle, which is incorporated via the Heaviside function $U(S_{k-1}^{min} - S_k^{min})$. Note that the overload excitation and reverse plastic flow are mutually exclusive.

The dimensionless parameter η in Eq. (9) depends on the specimen thickness t, half-width w, yield strength S^y, and Young's modulus E. Following an overload cycle, the duration of crack retardation is controlled by the transient of S_k^o in the state-space model, and hence determined by the stress-independent parameter η in Eqs. (8) and (9). Physically, this duration depends on the ductility of the material that is dependent on many factors including the heat treatment of specimens [11]. Smaller yield strength produces a smaller value of η, resulting in longer duration of the overload effect. Smaller specimen thickness has a similar effect [11]. Although a precise relationship for η is not known at this time due to the lack of adequate test data for different materials, η may be estimated from a single overload data for another identical specimen made of the same material. In the absence of such data, the relationship in Eq. (9) could be used to generate an estimate of η.

Next, we address the issue of (possibly) additional delays associated with the transient response of crack opening stress S_k^o, which might be prevalent in some materials. In order to include the effects of delay ℓ (in cycles) in the response of S_k^{oss}, the right-hand side of Eq. (1) can be modified by altering ΔK_k^{eff} as:

$$\Delta a_k \equiv a_k - a_{k-1} = h\left((S_k^{max} - S_{k-\ell-1}^o)\sqrt{\pi a_{k-1}}F(a_{k-1})\right) \text{ with } S_{k-\ell-1}^o = S_k^{min} \quad \text{for } \ell \geq 0 \tag{10}$$

Since the experimental data may not exactly show the transients of S^o during and immediately after a variation of S^{max} or S^{min}, the model may not accurately depict S^o in this range. Nevertheless, this (possible) modeling inaccuracy has hardly any effect on overall crack growth. Starting with a higher order difference equation, the order (i.e., the number of state variables) of the present model is reduced to 2 by singular perturbation [26] based on the experimental data of 7075-T6 [9] and 2024-T3 [10] aluminum alloys. The possibility of a higher order model to represent non-minimum phase behavior or delayed response of S_k^o is not precluded for other materials.

Remark 2.4. Eq. (10) *is identical to* Eq. (1) *for* $\ell = 0$. *In that case, the transient response of crack growth is subjected to a built-in delay of two cycles after the application of an overload pulse as seen by examination of* Eqs. (1) and (8). *For* $\ell > 0$, *the corresponding delay is* $(\ell + 2)$ *cycles.*

2.1. Features of the state-space model

The most important feature of the state-space model is recursive computation of the crack opening stress without the need for information storage of stress excitation except for the minimum stress in the previous cycle. This is evident from the governing Eqs. (1) and (8) for a_k and S_k^o, respectively, that the two-dimensional state-space model of fatigue crack growth has the structure of an ARMA model [6]. In other words, the crack growth equations can be represented by a second order nonlinear difference equation that recursively updates the state variables, a_k and S_k^o, with S_k^{max}, S_k^{min} and S_{k-1}^{min} as inputs and the immediate past information on a_{k-1} and S_{k-1}^o; storage of no other information is required. This implies that the crack length and crack-opening stress in the present cycle are obtained as simple algebraic functions of the maximum and minimum stress in the present cycle as well as the minimum stress, crack length, and crack-opening stress in the immediately preceding cycle.

Next, we compare the state-space model (which is ARMA) with the autoregressive (AR) model proposed by Holm et al. [27]. While both models are piecewise linear and treat the crack-opening stress S^o as a state variable, there are several differences in the structures of their governing equations. Specifically, the state-space model uses mechanistic principles and takes advantage of fatigue test data, while the AR model is largely empirical. The phenomenon of crack growth retardation requires only one constant parameter η in the state-space model. The AR model uses different constant parameters over the two halves of a cycle to represent the increase and decrease of S_k^o. A major drawback of having two different constants is that when frequent overloads (or underloads) are applied, S_k^o rises with each successive application and becomes unbounded. Consequently, the AR model is not capable of capturing the effects of a single overload, irregular load sequences, and random loads with the same set of constants. This problem does not arise in the state-space model as the excitation S_k^{oss} applied due to an overload is automatically adjusted by subtracting the current value of S_k^o as seen in the third term on the right hand side of Eq. (8). The effects of an abrupt reduction in S^{min} during the crack retardation period are realized in the fourth term.

3. Model validation with fatigue test data

This section validates the state-space model with the fatigue test data of: (i) 7075-T6 aluminum alloy specimens under different types of variable amplitude cyclic loading [9]; and (ii) 2024-T3 aluminum alloy specimens under spectrum loading [10]. Predictions of the state-space model and the FASTRAN-II model [2] are compared with the test data. The state-space model predictions are also comparable with those of other (crack-tip plastic-zone-based) models (e.g., Wheeler, Willenborg, and Chang) that are available in the AFGROW software package [3]. These results are not presented in this paper as they do not convey any significant new information.

3.1. Validation of the state-space model with Porter data

Porter [9] collected fatigue test data on center-notched 7075-T6 aluminum alloy specimens made of 305 mm wide, 915 mm long, and 4.1 mm thick panels, for which $E = 69{,}600$ MPa, $\sigma^y = 520$ MPa, and $\sigma^{ult} = 575$ MPa. The initial crack size ($2a$) was 12.7 mm and the experiments were conducted in laboratory air. Table 1 provides the lookup table data for $h(\cdot)$ in Section 2, which is used instead of the closed form expression $C(\Delta K_k^{eff})^m$, to generate predictions of both the state-space and FASTRAN-II models. Table 2 lists the parameters, α^{max}, α^{min}, Δa^{max} and Δa^{min} for updating the constraint factor α_k by interpolation (FASRAN-II manual, [2, p. 62]). Note that α_k varies between 1.1 and 1.8 for ductile alloys, depending on the instantaneous crack increment Δa_k. Fig. 1 shows the profile of block loading

Table 1
Crack growth lookup table for 7075-T6

ΔK^{eff} (MPa $\sqrt{m}$)	Crack growth rate (m/cycle)
0.90	1.0×10^{-11}
1.35	1.2×10^{-9}
3.40	1.0×10^{-8}
5.20	1.0×10^{-7}
11.9	1.0×10^{-6}
18.8	1.0×10^{-5}
29.0	1.0×10^{-4}

for data generation where the positive integers, n and m, indicate that a block of n constant-amplitude cycles is followed by a larger amplitude block of m cycles. Using the relationship $\eta \equiv tS^y/2wE$ in Section 2, the parameter η is evaluated to be $\sim 10^{-4}$ for the Porter specimen. Since η is stress-independent, this specific value is used for model validation under different loading conditions of Porter data.

Fig. 2 shows a comparison of the state-space model predictions with Porter data and the predictions of FASTRAN-II model that calculates the crack opening stress S^o in a different way. The curves in the top left corner plate in Fig. 2 are generated at n = 0 and m = 50 implying that the load is of constant-amplitude load with peak $\sigma_2 = 103.5$ MPa (15 ksi). The state-space and FASTRAN-II models produce essentially identical results under constant-amplitude cyclic stresses, because the procedure for calculating S^{oss} is similar in both models. The curves in each of the remaining plates in Fig. 2 are generated with the parameter n = 50 and the peak stress of overload $\sigma_2 = 103.5$ MPa (15 ksi) at different values of m in the load spectrum of Fig. 1. The analyses on both FASTRAN-II and the state-space models have been conducted with identical initial crack length with the assumption of no loading history. Therefore, the initial value of S^o is not assigned. For variable-amplitude cyclic stresses, the state-space model predictions are quite close to both the experimental data and predictions of the FASTRAN-II model, as seen in Fig. 2.

Predictions of both models are compared with Porter data in Fig. 3 for different amplitudes of single-cycle overload with m = 1 and n = 29 for different overload stress ratios σ_2/σ_1, while σ_1 is held fixed at 69 MPa (10 ksi). Similar comparisons are made in Fig. 4 for single-cycle overload (i.e., m = 1) with different values of overload spacing n and fixed values of $\sigma_2 = 103.5$ MPa (15 ksi) and $\sigma_1 = 69$ MPa (10 ksi). The plots in Figs. 3 and 4 indicate that the accuracy of the state-space model relative to the experimental data is comparable to that of the FASTRAN-II model. As seen in Figs. 5 and 6, the state-space model demonstrates the difference between the effects of overload-underload and underload-

Table 2
Model parameters for fatigue crack growth in aluminum alloys

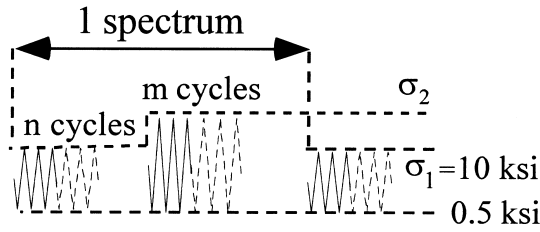| Alloy	α^{max}	α^{min}	Δa^{max}	Δa^{min}	C	m
7075-T6	1.8	1.1	5×10^{-6}	5×10^{-5}	(See Table 1)	
2024-T3	1.73	1.1	9×10^{-8}	7.5×10^{-7}	5×10^{-11}	4.07

Fig. 1. Cyclic stress excitation for Porter data.

overload on crack growth in agreement with the test data. In contrast, the FASTRAN II model does not show any appreciable difference when corresponding results are compared. The predictions of the state-space model are apparently superior to those of FASTRAN II for sequence effects.

3.2. Predictions for complex spectrum loads

McMillan and Pelloux [10] collected fatigue data under complex spectrum loads for center-notched 2024-T3 aluminum alloy specimens made of 229 mm wide, 610 mm long and 4.1 mm thick panels. Fatigue testing was accomplished in a vertical 125 kip electro-hydraulic fracture jig of Boeing design. The testing system was capable of applying loads with an absolute error within $\pm 1\%$ of the maximum programmed load. The initial crack size ($2a$) was 12.7 mm and the experiments were conducted in laboratory air. Thirteen load spectrum programs, P1–P13 were run on different specimen until failure. The composition of the 2024-T3 alloy used for spectra P1–P7 and P11–P13 was slightly different from that of the 2024-T3 alloy used for spectra P8–P10. The average properties of both materials based on three observations are listed in Table 3. The Young's modulus of 2024-T3 alloy is 71,750 MPa. Fatigue crack growth for spectra P1–P13 is calculated based on the parameters of 2024-T3 alloy in Table 2 and the closed form $C(\Delta K_k^{\text{eff}})^m$ of the function $h(\cdot)$ in Section 2. Using the relationship $\eta = tS^y/2wE$ in Section 2, the parameter η is evaluated to be $\sim 0.78 \times 10^{-4}$ for spectra P8–P10 and $\sim 0.82 \times 10^{-4}$ for the remaining spectra based on the material parameters in Table 3.

Predictions of the specimen life for the state-space and FASTRAN-II models are compared with test data of McMillan and Pelloux [10] for each load spectrum as shown as shown in Table 4. In view of the fact that the number of samples (e.g., in the order of three or four) over which the test data are averaged is small, modest disagreements (in the range of $\sim 10\%$) between the state-space model predictions and the test data in Table 4 are reasonable. Although both state-space and FASTRAN-II

Table 3
Average properties of 2024-T3 used under load spectra[a]

Spectrum program	Ultimate strength σ^{ult} (MPa)	Yield strength σ^y (MPa)
P1–P7, P11–P13	473.3	327.9
P8–P10	492.1	315.1

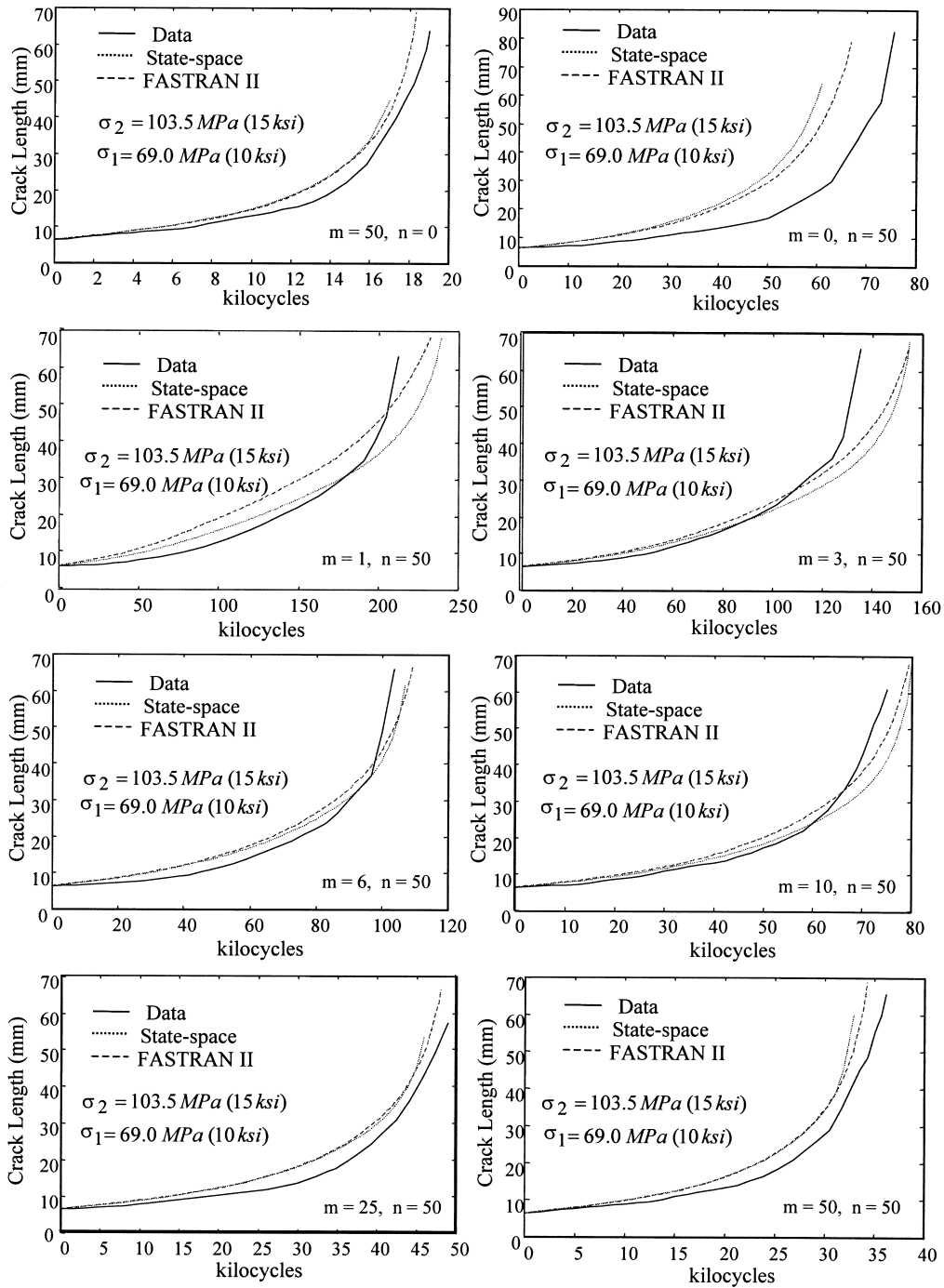[a] Young's Modulus $E = 71{,}750$ MPa for spectrum programs P1–P13.

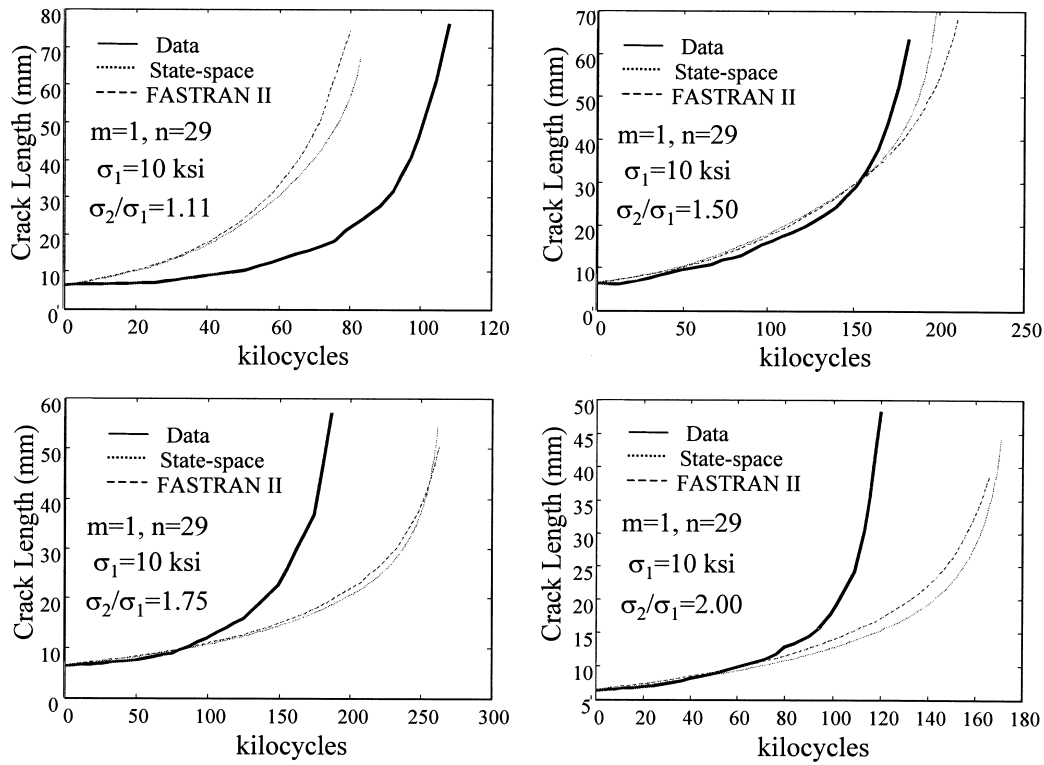Fig. 2. Model validation with Porter data under block loading.

Fig. 3. Model validation with Porter data under different overload amplitude.

Table 4
Comparison of predicted and actual life under spectrum loads

Program spectrum	Specimen life in number of spectra		
	Test data	State-space model prediction	FASTRAN-II model prediction
P1	4950	4542	3018
P2	5330	4583	3135
P3	3630	3375	2693
P4	1875	1667	1282
P5	3605	3125	2470
P6	10775	9091	8550
P7	11900	9636	8463
P8	3860	3438	2211
P9	3700	2813	2206
P10	2553	1677	1691
P11	7900	6990	5138
P12	5060	4625	2560
P13	2680	2450	1653
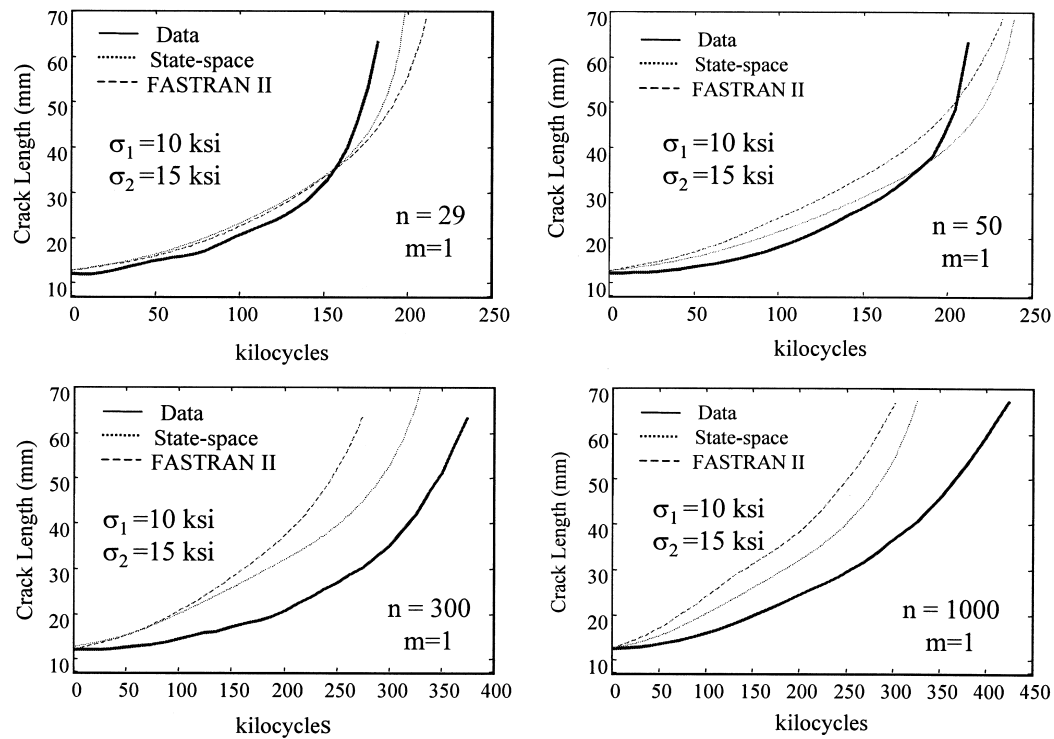
Fig. 4. Model validation with Porter data under different overload spacings.

Table 5
Execution time on 200 MHz Intel Pentium PC platform

Load description	State-space model (time in seconds)	FASTRAN-II Model (time in seconds)
Program P1	2.13	12.53
Program P2	2.1	13.99
Program P3	1.55	17.45
Program P4	1.53	12.49
Program P5	1.75	16.89
Program P6	4.04	18.04
Program P7	4.08	18.22
Program P8	3.14	19.79
Program P9	2.54	22.13
Program P10	1.83	19.75
Program P11	3.41	16.35
Program P12	2.09	19.47
Program P13	2.07	15.95

models yield acceptable results, predictions of the state-space model are closer to the experimental data in almost all thirteen cases of spectrum loads P1–P13 as seen in the plates of Figs. 7–10. The agreement of state-space model predictions with experimental data strongly supports the fundamental hypothesis that the crack opening stress can be treated as a state variable.
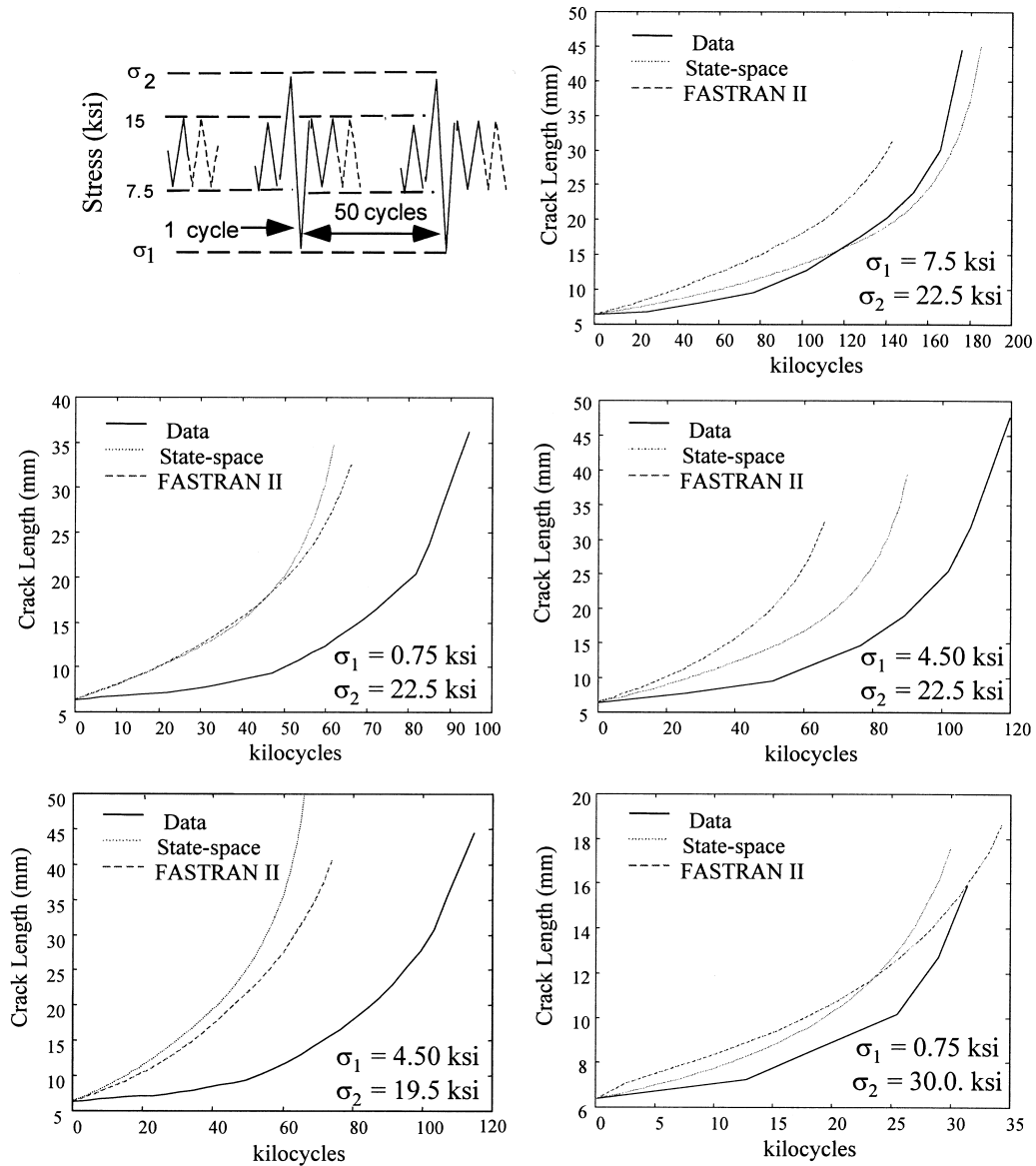
Fig. 5. Model validation with Porter data (overload-underload).

4. Comparison of computation time

Table 5 lists typical computation time required for calculation of crack growth under programmed loads P1–P13 on a 200 MHz Intel Pentium PC platform. A similar comparison for Porter data has been reported earlier by Patankar et al. [28] on an SGI Indy platform. In most of the thirteen cases reported in Table 5, the state-space model predicts a longer life than FASTRAN II by a few thousand cycles. In
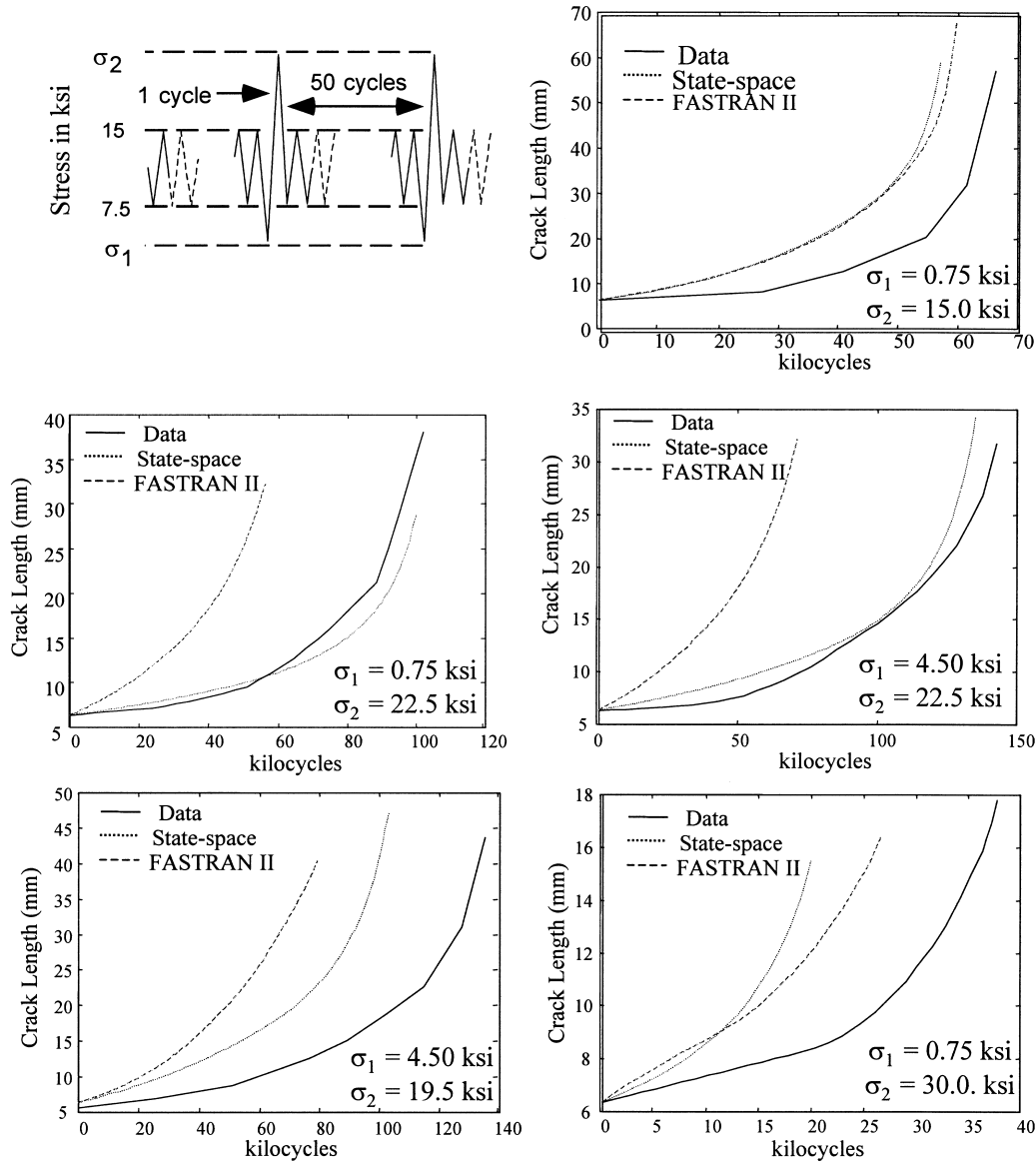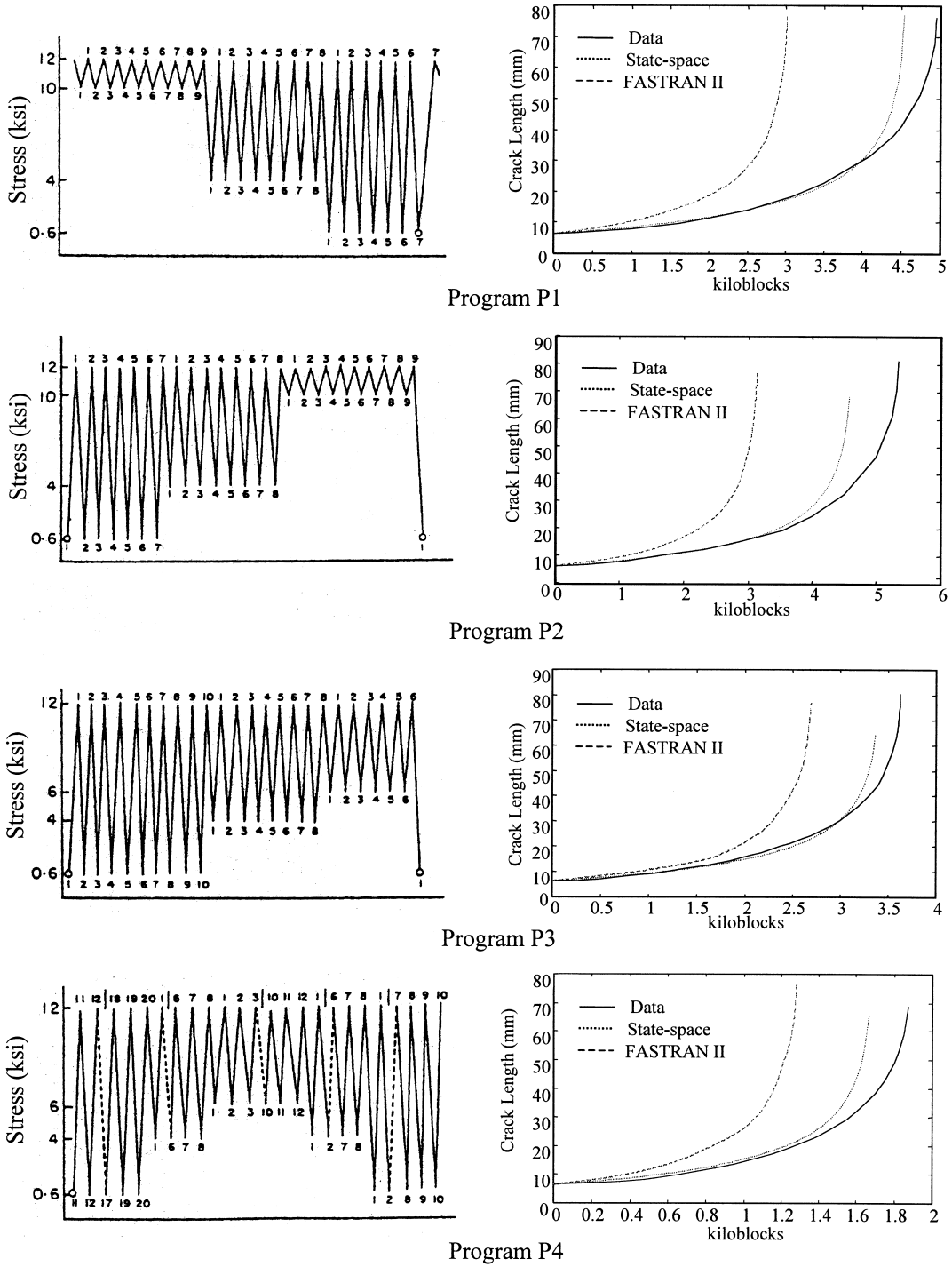

Fig. 6. Model validation with Porter data (underload-overload).

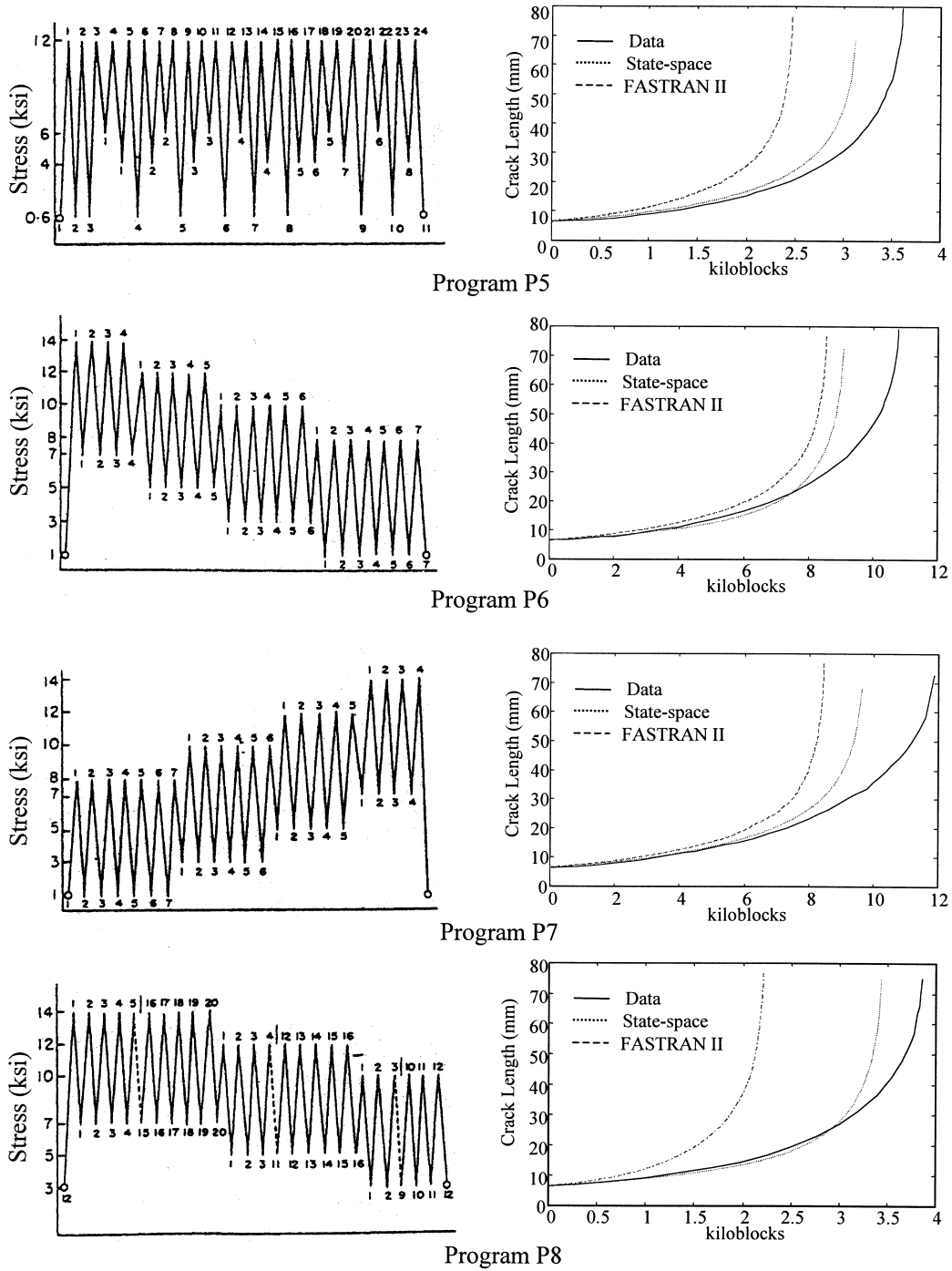Fig. 7. Model validation with spectral data (programs P1–P4).

Fig. 8. Model validation with spectral data (programs P5–P8).
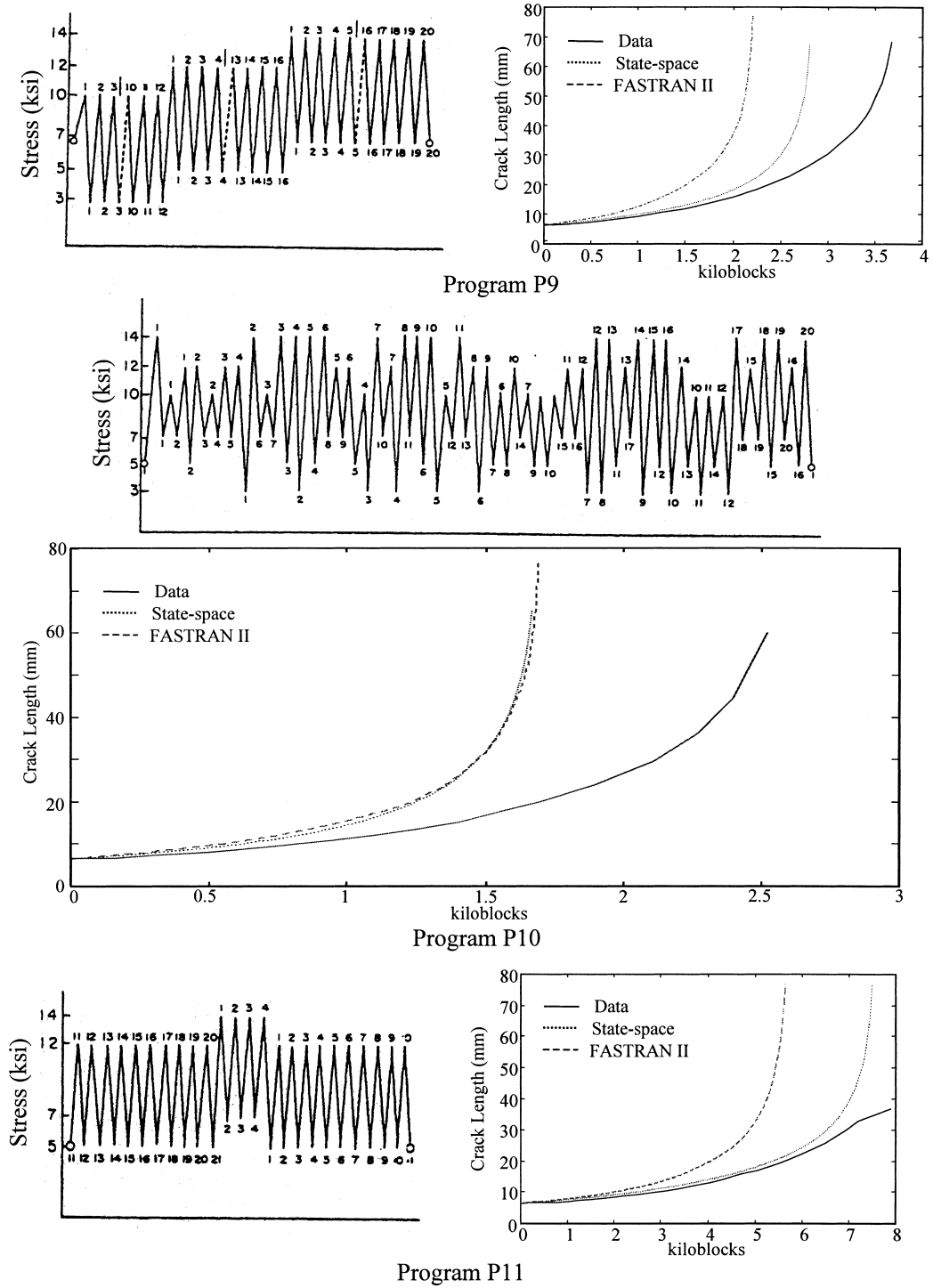
Program P9

Program P10

Program P11

Fig. 9. Model validation with spectral data (programs P9–P11).
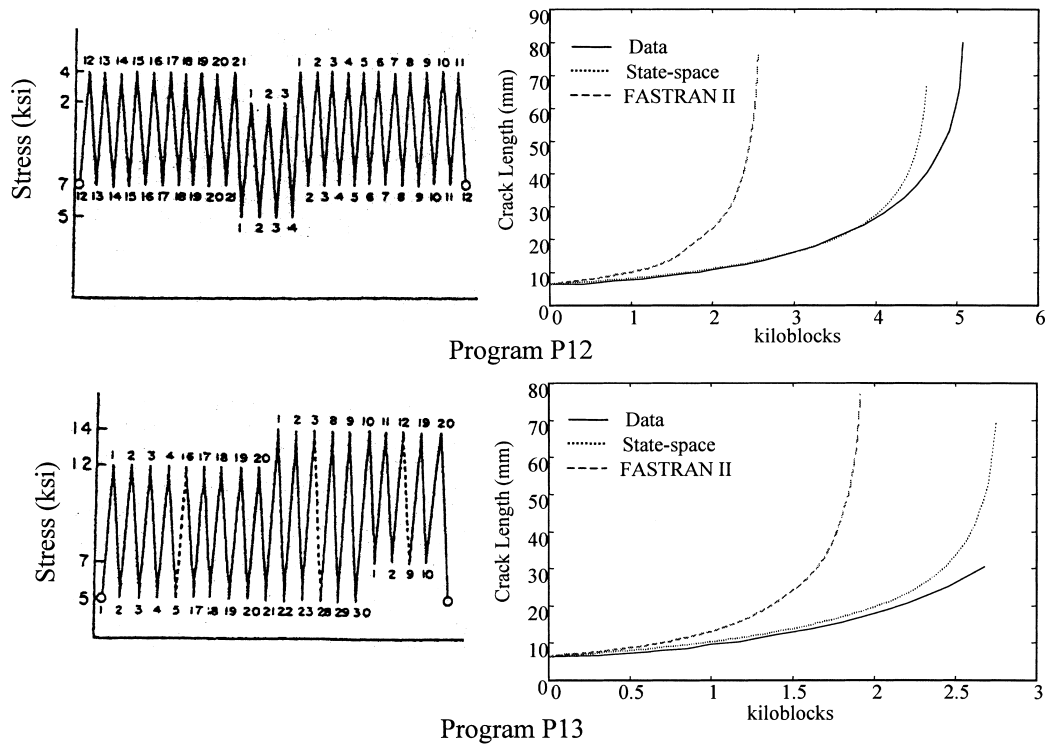
Fig. 10. Model validation with spectral data (programs P12 and P13).

the case of spectrum P10, both models run for approximately the same number of cycles, which provides a fair comparison of their computation time. The state-space model is more than 10 times faster than the FASTRAN II model for the spectrum P10. The execution time per spectrum block for both the models indicates that the state-space model is about 10 times faster than the FASTRAN II model for each of the thirteen spectrums. The rationale for significantly enhanced computational performance of the state-space model is given below.

The state-space model recursively computes S_k^o with S_k^{max}, S_k^{min} and S_{k-1}^{min} as inputs, as seen in Section 2. This implies that the crack opening stress in the present cycle, is obtained as a simple algebraic function of the maximum and minimum stress excitation in the present cycle, as well as the minimum stress and the crack opening stress in the immediately preceding cycle. In contrast, the FASTRAN-II model computes the crack opening stress as a function of contact stresses and crack opening displacements based on the stress history.

Since the state-space model does not need storage of load history except the minimum stress in the previous cycle, its memory requirements are much lower than those of FASTRAN II that does require storage of a relatively long load history. Consequently, both computer execution time and memory requirement of the state-space model are significantly smaller than those of the FASTRAN-II model. Specifically, the state-space enjoys the following advantage over other crack growth models:

- smaller execution time and computer memory requirements as needed for real-time heath monitoring and life extending control [29]; and

● Compatibility with other state-space models of plant dynamics (e.g., aircraft flight dynamic systems and rocket engine systems) and structural dynamics of critical components as needed for synthesis of life-extending control systems [8].

5. Summary and conclusions

This paper presents formulation and validation of a state-space model for fatigue crack growth prediction under variable-amplitude loading. The state-space model is built upon fracture-mechanistic principles of the crack-closure concept and experimental observations of fatigue test data. The model state variables are crack length and crack opening stress, and the model inputs are maximum stress and minimum stress in the current cycle and the minimum stress in the previous cycle. As such the crack growth model can be represented in the ARMA setting by a second order nonlinear difference equation that recursively computes the state variables without the need for storage of stress history except the minimum and maximum stresses in the present cycle and the minimum stress in the immediate past cycle. The two-state model can be augmented with additional states to capture the delayed effects of crack retardation if necessary. Simplistic state-space models, meant for constant-amplitude loads [8,29,30], have been used earlier for monitoring and control applications because of unavailability of a reliable model for crack growth prediction under variable-amplitude load. With the availability of the state-space model, reliable strategies can now be formulated for real-time decision and control of damage-mitigation and life-extension.

Although the structure of the state-space model for crack growth prediction is similar to that of the FASTRAN-II model [2], the major difference is in the formulation of transient behavior of the crack opening stress. Since the crack opening stress in FASTRAN-II is calculated asynchronously based on a relatively long history of stress excitation over the past (~300) cycles, it does not follow a state-space structure. The state-space model of fatigue crack growth adequately captures the effects of stress overload and reverse plastic flow, and is applicable to various types of loading including single-cycle overloads, irregular sequences and random loads. The state-space model has been validated with fatigue test data of Porter [9] and McMillan and Pelloux [10] for 7075-T6 and 2024-T3, respectively. The model predictions are also compared with those of FASTRAN-II for identical input stress excitation. While the results derived from these two models are comparable, the state-space model enjoys significantly smaller computation time and memory requirements.

The state-space model uses the structure of constant-amplitude crack opening stress [23] as a forcing function into the constitutive equation of crack opening stress. Construction of a state-space model based on other forcing functions needs to be explored.

Although the constitutive equation for crack opening stress in the state-space model is built upon physical principles, the model formulation still relies on semi-empirical relationships derived from experimental data. More emphasis on the physics of fatigue fracture will enhance the credibility of the state-space model; and also expose its potential shortcomings, if any. Therefore, it is desirable to formulate the transient behavior of the crack opening stress in the microstructural setting based on the dislocation theory.

Currently, the transients of crack opening stress are estimated from the available fatigue test data of crack growth. The information on relatively fast dynamics of crack opening stress is likely to be contaminated during the estimation process. Transient test data on crack opening stress under load variations are necessary for identification of more accurate and reliable state-space models. Controlled experiments, equipped with high-bandwidth instrumentation, need to be carried out to determine the

exact nature of nonlinearities that are represented by the Heaviside functions in the state-space model. Availability of additional crack growth data, under different types of cyclic loads and for different materials and specimen geometry, will enhance validation of the state-space model.

Acknowledgements

References

[1] Paris PC, Erdogan F. A critical analysis of crack propagation laws. Journal of Basic Engineering, ASME Trans 1960;85:528–34.

[2] Newman Jr., JC. FASTRAN-II — a fatigue crack growth structural analysis program. NASA Technical Memorandum 104159, Langley Research Center, Hampton, VA 23665.

[3] Harter JA. AFGROW Users' guide and technical manual. Report No. AFRL-VA-WP-1999-3016, Air Force Research Laboratory, WPAFB, OH 45433–7542.

[4] Dowling NE. Fatigue life prediction for complex load versus time histories. Journal of Engineering Materials and Technology, ASME Trans 1983;105:206–14.

[5] Rychlik I. Note on cycle counts in irregular loads. Fatigue and Fracture of Engineering Materials and Structures 1993;16(4):377–90.

[6] Ljung L. System identification theory for the user, 2nd ed. Englewood Cliffs, NJ: Prentice Hall, 1999.

[7] Newman Jr., JC. A crack-closure model for predicting fatigue crack growth under aircraft loading. Methods and Models for Predicting Fatigue Crack Growth under Random Loading. ASTM STP 748, 1981, pp. 53–84.

[8] Ray A, Wu M-K, Carpino M, Lorenzo CF. Damage-mitigating control of mechanical systems: Parts I and II. Journal of Dynamic Systems, Measurement and Control, ASME Trans 1994;116(3):437–55.

[9] Porter TR. Method of analysis and prediction for variable amplitude fatigue crack growth. Engineering Fracture Mechanics 1972;4:717–36.

[10] McMillan JC, Pelloux RMN. Fatigue crack propagation under program and random loads. Fatigue Crack Propagation. ASTM STP 415. 1967, pp. 505–32 (Also BSRL Document D1-82-0558, 1966).

[11] Schijve J. Observations on the prediction of fatigue crack growth propagation under variable-amplitude loading. Fatigue Crack Growth under Spectrum Loads. ASTM STP 595, 1976, pp. 3–23.

[12] Anderson TL. Fracture mechanics, 2nd ed. FL: CRC Press, 1995.

[13] Schijve J, Jacobs FA, Tromp PJ. The effect of load sequence under fatigue crack propagation under random loading and program loading. NLR TR 71014 U, National Aerospace Laboratory NLR, The Netherlands, 1971.

[14] Jacoby GH, Van Lipzig HTM, Nowack H. Experimental results and a hypothesis for fatigue crack propagation under variable amplitude loading. Fatigue Crack Growth under Spectrum Loads. ASTM STP 595, 1976, pp. 172–183.

[15] Schijve J. Fatigue damage accumulation and incompatible crack front orientation. Engineering Fracture Mechanics 1974;6:245–52.

[16] Sharpe Jr., WN, Corbly DM, Grandt AF Jr., Effects of rest time on fatigue crack retardation and observation of crack closure. Fatigue Crack Growth under Spectrum Loads, ASTM STP 595, 1976, pp. 61–77.

[17] Yisheng W, Schijve J. Fatigue crack closure measurements on 2024-T3 sheet specimens. Fatigue and Fracture of Engineering Materials and Structures 1995;18(9):917–21.

[18] Newman Jr, JC. Prediction of fatigue crack growth under variable-amplitude and spectrum loading using a closure model. Design of Fatigue and Fracture Resistant Structures. ASTM STP 761, 1982, pp. 255–277.

[19] Dabayeh AA, Topper TH. Changes in crack-opening stress after underloads and overloads in 2024-T351 aluminium alloy. International Journal of Fatigue 1995;17(4):261–9.

[20] Suresh S. Fatigue of materials. Cambridge, UK: Cambridge University Press, 1991.

[21] Vidyasagar M. Nonlinear systems analysis, 2nd ed. Englewood Cliffs, NJ: Prentice Hall, 1992.

[22] Lardner RW. Mathematical theory of dislocations and fracture. Toronto, Canada: University of Toronto Press, 1974.

[23] Newman Jr JC. A crack opening stress equation for fatigue crack growth. International Journal of Fracture 1984;24:R131–R135.

[24] Ibrahim FK, Thompson JC, Topper TH. A study of effect of mechanical variables on fatigue crack closure and propagation. International Journal of Fatigue 1986;8(3):135–42.

[25] Patankar R. Modeling fatigue crack growth for life-extending control. Ph.D. Dissertation, Department of Mechanical Engineering, The Pennsylvania State University, University Park, PA, May 1999.

[26] Kokotovic P, Khalil HK, O'Reilly J. Singular perturbation methods in control analysis and design. London, UK: Academic Press, 1986.

[27] Holm S, Josefson BL, de Mare J, Svensson T. Prediction fatigue life based on level crossings and a state variable. Fatigue and Fracture of Engineering Materials 1995;18(10):1089–100.

[28] Patankar R, Ray A, Lakhtakia A. A state-space model of fatigue crack growth. International Journal of Fracture 1998;90(3):235–49.

[29] Holmes M, Ray A. Fuzzy damage mitigating control of mechanical structures. ASME Journal of Dynamic Systems, Measurement and Control 1998;120(2):249–56.

[30] Lorenzo CF, Holmes M, Ray A. Design of life extending control using nonlinear parameter optimization. Lewis Research Center Technical Report No. NASA TP 3700, 1988.